THE ASTROPHYSICAL JOURNAL, 339:339–353, 1989 April 1

MODELING "HYDRODYNAMIC PHASE TRANSITIONS" IN A RADIATING SPHERICALLY SYMMETRIC DISTRIBUTION OF MATTER

L. HERRERA
Departamento de Física, Facultad de Ciencias, Universidad Central de Venezuela

AND

L. NÚÑEZ
Departamento de Física, Facultad de Ciencias, Universidad Central de Venezuela; and Laboratorio de Física Teórica, Departamento de Física, Facultad de Ciencias, Universidad de Los Andes

Received 1988 March 22; accepted 1988 September 7

ABSTRACT

A method recently proposed by the authors to study the evolution of discontinuities in radiating spherically symmetric distributions of matter is extended to model "hydrodynamic phase transitions" in a composite radiant sphere. The matter configuration is divided into two regions by a shock wave front, and at each side of this interface a different anisotropic phase is considered. Solutions are matched across the shock via the Rankine-Hugoniot conditions, while the outer region metric joins the Vaidya solution at the boundary surface. The matter distribution is free of singularities within the sphere, and a Gaussian-like radiation pulse is assumed to carry out a fraction of the total mass. The resulting models strongly depend on the anisotropic jump across the interface and on the luminosity (opacity) of the shock wave. Finally, prospective applications to astrophysical scenarios are discussed.

Subject headings: dense matter — hydrodynamics — shock waves — stars: neutrons

I. INTRODUCTION

Strong theoretical evidence suggests that, at least for a certain density range, exotic phase transitions may occur during the process of gravitational collapse (Collins and Perry 1975; Itoh 1970; Migdal 1971; Sawyer 1972; Sokolov 1980). Particularly noticeable are transitions to a pion condensed state which, softening the equation of state (Hartle, Sawyer, and Scalapino 1975) and providing an enormous release of energy (Sawyer and Soni 1977), have important implications in the evolution of collapsing configurations. Although these features indicate a possible connection with a supernova scenario (Migdal, Chernoutsan, and Mishustin 1979), this process seems to be not energetic enough to be considered as an alternative framework to explain a supernova outburst (Haensel and Prószyński 1980; Kampfer 1985; Takahara and Sato 1985). Nonetheless, it may be considered as an efficient cooling mechanism at the early stages of neutron star evolution (Maxwell 1987; Maxwell *et al.* 1977). It is interesting to note that this phase transition gives rise to a large moving density discontinuity which could be treated as a shock wave (Migdal, Chernoutsan, and Mishustin 1979), and, as stated by Hartle, Sawyer, and Scalapino (1975), it may be of possible significance in theories of neutron starquakes.

Early in the last decade Sawyer and Scalapino (1973) pointed out that, because of the geometry of the π^- modes, anisotropic distributions of pressure could be considered to describe a pion condensed phase configuration. Anisotropic matter representing this and other interesting physical situations, e.g., the existence of a solid core (Ruderman 1972), the presence of a type P superfluid, or the use of a two-fluid model for noninteracting perfect fluids (Canuto 1973; Letelier 1980), is now thought to be the constituent of more realistic compact objects. This possibility of introducing important physical phenomena in a very simple and elegant way opens a wide opportunity to obtain physically interesting interior solutions of the Einstein field equations.

Since the pioneering work of Bowers and Liang (1974), the influence of local anisotropy in general relativity has been extensively studied. We present a brief summary of the state of the art regarding anisotropy within the context of interior solutions in general relativity. Analytical static solutions were studied by Bayin (1982), Cosenza *et al.* (1981), Heintzmann and Hillebrandt (1975), Herrera and Ponce de León (1985*a*, *b*), Krori, Borgohain, and Devi (1984), and Ponce de León (1987). Hillebrant and Steinmetz (1976) analyzed the problem of the stability of an anisotropic neutron star in the presence of radial pulsations. Herrera, Ruggeri, and Witten (1979) devoted their work to examining the slow adiabatic contraction of an anisotropic sphere. Cosenza *et al.* (1982), Esculpi and Herrera (1986), and Ibáñez (1984) studied the evolution of radiating anisotropic fluid spheres. Ibáñez and Miralles (1985) pointed out several influences of anisotropy upon white dwarf collapse. Bayin (1982) additionally considered the collapse of radiating slowly rotating anisotropic spheres. Some geometrical aspects of spacetime, anisotropy, and its hydrodynamic implications were recently presented by Duggal (1987), Duggal and Sharma (1986), Herrera *et al.* (1984), and Maartens, Mason, and Tsamparlis (1986). The role played by anisotropy in the context of other gravitational theories had been investigated by Ram and Pandey (1986).

Recently, the propagation of discontinuities in a one–isotropic-phase radiating sphere has been considered (Herrera and Núñez 1987). In the present paper we extend this method to the case of a composite two–anisotropic-phase matter configuration. The sphere is divided into two regions by a shock wave front, and at each side of the shock a different anisotropic phase is considered. The solutions corresponding to either side of the front are matched across it via the Rankine-Hugoniot conditions (Taub 1948,

1983; Herrera and Núñez 1987). The matching with the Vaidya metric on the boundary of the sphere completes the consistency of this description.

Following our previous work (Herrera and Núñez 1987), a heuristic assumption relating pressure, energy density, and the radial velocity of matter is introduced. This *Ansatz*, together with the junction conditions at the shock and at the boundary of the matter distribution, leads to a system of ordinary differential equations for quantities evaluated at either the boundary surface or the shock front. Thus, the numerical integration of this system allows us, using the field equations, to find the profile of the physical variables throughout.

In the particular example worked out in this paper the solution describing the composite anisotropic sphere is a generalization of the nonstatic and radiating Schwarzschild interior metric for both isotropic and anisotropic fluids (Cosenza *et al.* 1982; Herrera, Jiménez, and Ruggeri 1980). The influence of the coexistence of these two phases on the collapse of the sphere is analyzed, carrying out the evolution for different anisotropic phase configurations at the core and at the mantle.

The paper is organized as follows. In § II the Einstein equation for the anisotropic case, as well as the conventions used, are introduced. The Rankine-Hugoniot conditions and an outline of method are presented in § III. In § IV the model is developed, and the results are discussed in § V. Finally, some details of intermediate calculations are sketched in the Appendix.

II. FIELD EQUATIONS AND GENERAL CONSIDERATIONS

Let us consider a nonstatic distribution of matter which is spherically symmetric. In radiation coordinates (Bondi 1964) the metric takes the form

$$ds^2 = e^{2\beta}[(V/r)du^2 + 2du\,dr] - r^2(d\theta^2 + \sin^2\theta\, d\varphi^2)\,, \tag{1}$$

where β and V are functions of u and r. Here $u \equiv x^0$ is a timelike coordinate, $r \equiv x^1$ is a null coordinate, and $\theta \equiv x^2$ and $\varphi \equiv x^3$ are the usual angle coordinates. In these coordinates the components of the energy momentum tensor are distinguished by means of a bar, while differentiation with respect to u and r is denoted by the suffixes 0 and 1, respectively.

Thus, it can be shown (Cosenza *et al.* 1982) that the Einstein equations may be written as

$$\frac{\rho + P\omega^2}{1-\omega^2} + \epsilon = \frac{r}{V}\,e^{-2\beta}\bar{T}_{00}\,,$$

$$= \frac{1}{4\pi r(r-2\tilde{m})}\left[-\tilde{m}_0\,e^{-2\beta} + \frac{r-2\tilde{m}}{r}\,\tilde{m}_1\right], \tag{2}$$

$$\frac{\rho - P\omega}{1+\omega} = e^{-2\beta}\bar{T}_{01} = \frac{\tilde{m}_1}{4\pi r^2}\,, \tag{3}$$

$$\frac{1-\omega}{1+\omega}(\rho + P) = \frac{V}{r}\,e^{-2\beta}\bar{T}_{11} = \frac{r-2\tilde{m}}{2\pi r^2}\,\beta_1\,, \tag{4}$$

$$P_\perp = -\bar{T}^2_2$$

$$= -\frac{\beta_{01}e^{-2\beta}}{4\pi} + \frac{1}{8\pi}\left(1-\frac{2\tilde{m}}{r}\right)\left(2\beta_{11} + 4\beta_1^2 - \frac{\beta_1}{r}\right) + \frac{3\beta_1(1-2\tilde{m}_1) - \tilde{m}_{11}}{8\pi r}\,, \tag{5}$$

where ρ, ω, P, and $P_\perp$ are respectively the energy density, the matter radial velocity, the radial pressure, and the tangential pressure as measured by a local Minkowski observer. Also the flux of radiation $\hat{\epsilon}$, as measured by the same observer, is related to ϵ by

$$\epsilon = \hat{\epsilon}\,\frac{1+\omega}{1-\omega}\,.$$

The field equations may be integrated outside the matter configuration to obtain

$$\beta = 0\,, \qquad V = r - 2m(u)\,, \qquad \epsilon = -\frac{m_0}{4\pi r(r-2m)}\,, \tag{6}$$

where m is a function of integration depending on u. Inside, the function $m(u)$ is generalized to $\tilde{m}(u, r)$ by setting

$$V = e^{2\beta}[r - 2\tilde{m}(u, r)] \tag{7}$$

everywhere. Also note that the velocity of matter in the radiative coordinates is given by

$$\frac{dr}{du} = \frac{V}{r}\,\frac{\omega}{1-\omega}\,. \tag{8}$$

Hence, in contrast to the isotropic case ($P_\perp \equiv P$), it is not sufficient to provide β and $\tilde{m}$ to calculate the physical variables. An equation of state relating the tangential pressure to the other dynamical quantities should be given. We shall return to this point in the discussion at the end of this section.

Let us define the two auxiliary functions

$$\tilde{\rho} \equiv \frac{\rho - \omega P}{1 + \omega}, \tag{9}$$

$$\tilde{P} \equiv \frac{P - \omega \rho}{1 + \omega}, \tag{10}$$

hereafter referred to as the effective density and the effective pressure, respectively. Observe that from the field equations (3) and (4) we have

$$\tilde{m} = \int_0^r 4\pi\tau^2 \tilde{\rho}\, d\tau, \tag{11}$$

$$\beta = \int_a^r \frac{2\pi\tau^2}{\tau - 2\tilde{m}} (\tilde{\rho} + \tilde{P})\, d\tau, \tag{12}$$

where $r = a(u)$ defines the boundary of the fluid sphere.

The main issue when introducing anisotropy is the choice of the equation of state relating the tangential pressure to the other dynamical variables. To infer this relation from physical grounds would be desirable, but at the present it is an extremely difficult task. Thus we shall follow the procedure introduced by Cosenza *et al.* (1982), where for the sake of mathematical simplicity the following equation of state is proposed:

$$P_\perp - P = \xi(\tilde{\rho} + \tilde{P}) \frac{\tilde{m}(u, r) + 4\pi r^3 \tilde{P}}{r - 2\tilde{m}(u, r)}, \tag{13}$$

where the parameter ξ characterizes the anisotropy of the configuration.

III. MATCHING ACROSS THE SHOCK AND OUTLINE OF THE METHOD

For completeness we outline here the matching conditions and the method presented in our previous paper (Herrera and Núñez 1987) extended to deal with anisotropy. Let us consider a sphere of radius $a(u)$ divided into two regions, say I and II, by a discontinuity surface (a shock) of radius $c(u)$ (see Fig. 1). Both $a(u)$ and $c(u)$ are functions of the timelike coordinate.

The matching conditions across the shock (the Rankine-Hugoniot conditions) require the continuity of the first and the second fundamental form plus the continuity of $T_{\mu\nu} n^\nu$, where $T_{\mu\nu}$ is the energy momentum tensor and n^ν is the unit vector normal to the

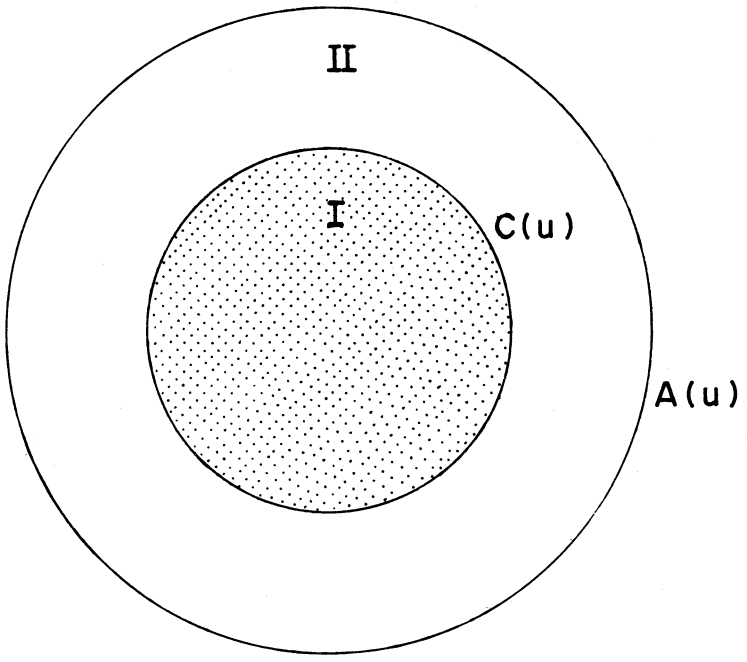

FIG. 1.—The two-region model sphere considered throughout this work. Region I, the inner core, is enclosed by a shock surface $C(u)$. The outer mantle completes the sphere of radius $A(u)$.

surface $r = c(u)$ (Taub 1948, 1983). The continuity of the first and second fundamental forms leads to the conditions (see Herrera and Jiménez 1983)

$$[\beta]_c = [\tilde{m}]_c = 0 \tag{14}$$

and

$$[2\beta_1 e^{2\beta}(1 - 2\tilde{m}/r) - 2\beta_0 - e^{2\beta}\tilde{m}_1/r]_c = 0 , \tag{15}$$

where

$$[f]_c \equiv f|_{r=c+0} - f|_{r=c-0} .$$

Next, since β is continuous across $c(u)$, equation (15) can be expressed as

$$\left[\frac{1-\omega}{1+\omega}(\rho + P)\Psi - \frac{\rho - \omega P}{1+\omega}\right]_c = 0 , \tag{16}$$

with

$$\Psi \equiv 1 + c_0 e^{-2\beta}(1 - 2\tilde{m}/r)^{-1} .$$

Finally, similar to the isotropic case, the conditions

$$[T_{\mu\nu} n^\nu]_c = 0 ,$$

are

$$\left[\frac{1-\omega}{1+\omega}(\rho + P)\Psi - \frac{\rho - \omega P}{1+\omega}\right]_c = 0 , \tag{17}$$

which is exactly condition (16) above, and

$$\left[\frac{\rho + \omega^2 P}{1-\omega^2} + \epsilon - \left(\frac{\rho - \omega P}{1+\omega}\right)\Psi\right]_c = 0 . \tag{18}$$

Let us now rewrite conditions (17) and (18) in terms of the effective variables. Using equations (9) and (10), we obtain

$$(1 - \Psi)[\tilde{\rho}]_c = \Psi[\tilde{P}]_c \tag{19}$$

and

$$[\Omega_s(\Omega_s - 1)(\tilde{\rho} + \tilde{P}) + (1 - \Psi)\tilde{\rho} + \epsilon]_c = 0 , \tag{20}$$

with $\Omega_s = 1/(1 - \omega_{c\pm 0})$. Also, using the field equations (3) and (4), we obtain for the metric functions β and $\tilde{m}$

$$m_I = \int_0^r 4\pi\tau^2\tilde{\rho}_I\, d\tau , \qquad 0 \le r \le c(u) , \tag{21}$$

$$\tilde{m}_{II} = \int_{c(u)}^r 4\pi\tau^2\tilde{\rho}_{II}\, d\tau + \tilde{m}_I(u, c(u)) , \qquad c(u) \le r \le a(u) , \tag{22}$$

and

$$\beta_I = \int_{c(u)}^r \frac{2\pi\tau^2}{\tau - 2\tilde{m}_I}(\tilde{\rho}_I + \tilde{P}_I)d\tau + \beta_{II}(u, c(u)) , \qquad 0 \le r \le c(u) , \tag{23}$$

$$\beta_{II} = \int_{a(u)}^r \frac{2\pi\tau^2}{\tau - 2m_{II}}(\tilde{\rho}_{II} + \tilde{P}_{II})d\tau , \qquad c(u) \le r \le a(u) , \tag{24}$$

where the subscripts I and II indicate the region the quantity is referred to. We can restate the algorithm for the composite anisotropic sphere as follows:

1. Take two static interior solutions of the Einstein equations for anisotropic fluids with spherical symmetry:

$$\rho_{st\,I} = \rho_I(r) , \qquad \rho_{st\,II} = \rho_{II}(r) ,$$
$$P_{st\,I} = P_I(r) , \qquad P_{st\,II} = P_{II}(r) .$$

2. Assume that the r-dependence of $\tilde{P}_{I,II}$ and $\tilde{\rho}_{I,II}$ is the same as that of $P_{st\,I,II}$ and $\rho_{st\,I,II}$, but taking account of the boundary condition, which, for this case, reads

$$\tilde{P}_{IIa} = -\omega_a \tilde{\rho}_{IIa} ,$$

and the conditions at $r = c(u)$ given by equations (19) and (20).

3. With the r-dependence of $\tilde{\rho}_{\mathrm{I,II}}$ and $\tilde{P}_{\mathrm{I,II}}$ and using equations (21)–(24), we obtain $\tilde{m}_{\mathrm{I,II}}$ and $\beta_{\mathrm{I,II}}$ up to some functions of u which will be specified below.

4. For these functions of u we obtain the following ordinary differential equations (surface equations). Three of them (two are model-independent) emerge as a consequence of the junction conditions and the field equations evaluated at the boundary surface. The remainder of the surface equations come from the Rankine-Hugoniot conditions.

a) The first equation comes from definition (8) evaluated at the boundary surface, which, after scaling the radius a, the total mass m, and the timelike coordinate u by the initial mass $m(u=0)\equiv m(0)$, that is

$$A\equiv a/m(0)\,,\qquad M\equiv m/m(0)\,,\qquad u/m(0)\to u\,,$$

and defining

$$F\equiv 1-2M/A\,,\qquad \Omega\equiv 1/(1-\omega_a)\,,$$

can be written as

$$\dot{A}=F(\Omega-1)\,. \tag{25}$$

b) The second surface equation relates the total mass-loss rate with the energy flux through the surface. This can be obtained by evaluating equation (2) for $r=a+0$ and takes the form

$$\dot{M}=-FE\,, \tag{26}$$

or, using the above definitions and equation (15),

$$\frac{\dot{F}}{F}=\frac{2E+(1-F)(\Omega-1)}{A}\,. \tag{27}$$

c) The third equation at the surface is obtained from the conservation equation $T^{\mu}{}_{1;\,\mu}=0$ evaluated at the surface. Thus, from

$$(T^{\mu}{}_{1;\,\mu})_a=0\,,$$

we obtain

$$-\left[\frac{\tilde{\rho}+\tilde{P}}{1-2\tilde{m}/r}\right]_{0a}+\left[\frac{\partial\tilde{P}}{\partial r}\right]_a+\left[\frac{\tilde{\rho}+\tilde{P}}{1-2\tilde{m}/r}\left(4\pi r\tilde{P}+\frac{\tilde{m}}{r^2}\right)\right]_a=\left[\frac{2}{r}(P_{\perp}-\tilde{P})\right]_a\,. \tag{28}$$

Notice that equations (26) and (27) are model-independent, while equation (28) should be particularly shaped for every model considered. If the effective density $\tilde{\rho}$ is separable, i.e.,

$$\tilde{\rho}=f(u)g(r)\,,$$

then, after a lengthy and tedious calculation, equation (28) becomes

$$\frac{\dot{F}}{F}+\frac{\dot{\Omega}}{\Omega}(1-F)=G(F,\Omega,A)\,, \tag{29}$$

with

$$G(F,\Omega,A)=(F-1)(\Omega-1)\left[4\pi a\tilde{\rho}_a\frac{3\Omega-1}{\Omega}+\frac{\Omega F\tilde{\rho}_{1a}}{\tilde{\rho}_a}-\frac{3+F}{2a}+\frac{2\Omega FP_{\perp a}}{a\tilde{\rho}_a}+K(a)F\right]-\frac{(1-F)\Omega^2FR_a(u)}{\tilde{\rho}_a}\,, \tag{30}$$

where

$$K(a)\equiv\frac{d}{da}\ln\left[\frac{1}{a}\int_0^a r^2\frac{g(r)}{g(a)}\,dr\right]\,,$$

and

$$R_a(u)=\left[\frac{\tilde{\rho}+\tilde{P}}{1-2\tilde{m}/r}\left(4\pi r\tilde{P}+\frac{\tilde{m}}{r^2}\right)+\frac{\partial\tilde{P}}{\partial r}-\frac{2}{r}(P_{\perp}-P)\right]_a\,.$$

(Note: the sign of the last two terms of eq. [30] appeared misprinted in the corresponding eq. [22] of Herrera and Núñez 1987.)

d) The remaining equations are also model-dependent and are written as a result of the matching conditions across $r=c(u)$.

5. Specifying the equation of state relating the tangential pressure with the other dynamical variables and providing three additional functions, one evaluated at $r=a(u)$ and the other two evaluated at $r=c(u)$, the complete system (25), (27), and (29) may be integrated for any particular set of initial data.

6. By substituting the result of the integration in the expressions for $\tilde{m}_{\mathrm{I,II}}$ and $\beta_{\mathrm{I,II}}$, these four functions become completely determined.

7. By using equations (2)–(5), the matter variables ρ, P, $P_{\perp}$, ω, and ϵ may be found for any part of the sphere.

In the above we have restated the outline of the general program for the attainment of anisotropic models. However, before discussing a specific example, two observations are in order:

i) Because of the large number of functions appearing in the system (25), (27), and (29), there are many ways to achieve step 5; the next section illustrates one of them. As will be seen there, the choice depends strongly on which are the observable functions of the process.

ii) The fact that two functions evaluated at $r = c(u)$ must be given by hand [in contrast to the situation at $r = a(u)$, where only one function of u has to be provided] is related to the continuity of the energy flux across the boundary surface $r = a(u)$; or equivalently, it is related to the fact that the shock velocity $\dot{c} = dc(u)/du$, is a new unknown function, since the matter velocity evaluated at the shock is not, in general, the velocity of the shock itself:

$$v|_{r=c} = \left[\frac{dr}{du}\right]_{r=c} \neq \frac{dc}{du} = \dot{c} .$$

IV. THE ANISOTROPIC COMPOSITE SPHERE

In this section we shall explicitly work out the formalism for studying the influence of the coexistence of two anisotropic phases on the evolution of a composite anisotropic sphere. In order to focus attention on this influence, and for the sake of simplicity, we shall assume the effective density to be the same across the shock, i.e.,

$$[\tilde{\rho}] \equiv 0 \leftrightarrow \tilde{\rho}_{\mathrm{Ic}} = \tilde{\rho}_{\mathrm{IIc}} = \tilde{\rho} , \tag{31}$$

and from equation (19) we find that

$$[\tilde{P}] = 0 \leftrightarrow \tilde{P}_{\mathrm{Ic}} = \tilde{P}_{\mathrm{IIc}} = \tilde{P}_{+} . \tag{32}$$

We consider a solution inspired by the anisotropic Schwarzschild interior solution (Cosenza *et al.* 1981, 1982):

$$\tilde{\rho} = f(u) , \qquad 0 \leq r \leq a(u) - 0 . \tag{33}$$

The effective pressure for the inner region $[0 \leq r \leq c(u) - 0]$ can be easily computed using equation (32):

$$\tilde{P}_{\mathrm{I}} = \tilde{\rho}\,\frac{(\tilde{\rho} + 3\tilde{P}_{+})(W^2 - r^2)^{k/2} - (\tilde{\rho} + \tilde{P}_{+})[W^2 - c(u)^2]^{k/2}}{3(\tilde{\rho} + \tilde{P}_{+})[W^2 - c(u)^2]^{k/2} - (\tilde{\rho} + 3\tilde{P}_{+})(W^2 - r^2)^{k/2}} , \tag{34}$$

while at the mantle $[c(u) \leq r \leq a(u) - 0]$ the boundary condition $\tilde{P}_{\mathrm{IIa}} = -\omega_a \tilde{\rho}_a$ leads to

$$\tilde{P}_{\mathrm{II}} = \tilde{\rho}\,\frac{(3 - 2\Omega)(W^2 - r^2)^{h/2} - [W^2 - a(u)^2]^{h/2}}{3[W^2 - a(u)^2]^{h/2} - (3 - 2\Omega)(W^2 - r^2)^{h/2}} , \tag{35}$$

with

$$W^2 = \frac{3}{8\pi f(u)} .$$

The parameters $k = 1 - 2\xi_{\mathrm{I}}$ and $h = 1 - 2\xi_{\mathrm{II}}$ characterize the anisotropy of the respective region. Equation (32) yields an expression for $\tilde{P}_{+}$, namely,

$$\tilde{P}_{+} = \tilde{\rho}\,\frac{(3 - 2\Omega)[W^2 - c(u)^2]^{h/2} - [W^2 - a(u)^2]^{h/2}}{3[W^2 - a(u)^2]^{h/2} - (3 - 2\Omega)[W^2 - c(u)^2]^{h/2}} . \tag{36}$$

The metric functions for this configuration become

$$\tilde{m} = \int_0^r 4\pi\tau^2\rho\, d\tau = \frac{r^3}{2W^2} , \tag{37}$$

$$\beta_{\mathrm{I}} = \frac{1}{2k}\ln\left|\frac{3(\tilde{\rho} + \tilde{P}_{+})[W^2 - c(u)^2]^{k/2} - (\tilde{\rho} + 3\tilde{P}_{+})(W^2 - r^2)^{k/2}}{2\tilde{\rho}(W^2 - r^2)^{k/2}}\right| + \frac{1}{2h}\ln\left|\frac{\tilde{\rho}(3 - 2\Omega)}{\Omega(\tilde{\rho} + 3\tilde{P}_{+})^{h/2}}\right| , \tag{38}$$

and

$$\beta_{\mathrm{II}} = \frac{1}{2h}\ln\left|\frac{3[W^2 - a(u)^2]^{h/2} - (3 - 2\Omega)(W^2 - r^2)^{h/2}}{2\Omega(W^2 - r^2)^{h/2}}\right| . \tag{39}$$

Note that both metric functions are coupled through the appearance of the function W^2 in equations (38) and (39).

Having specified the solutions (up to some functions of u) at either side of the shock, the surface equations can be written down. Three of them correspond to quantities evaluated on the surface at $r = a(u)$ (eqs. [25], [27], and [29]). The other one comes from the Rankine-Hugoniot condition expressed by equation (20). Using equations (31) and (32), it takes the form

$$[\Omega(\Omega - 1)]_c = \frac{-1}{\tilde{\rho}_c + \tilde{P}_c}\,[\epsilon]_c . \tag{40}$$

So far the set of unknown functions of u reduces to

$$A,\ F,\ \Omega,\ C,\ E,\ \Omega_{\rm I},\ \Omega_{\rm II},\ \epsilon_{\rm I},\ \epsilon_{\rm II}.$$

In order to find them, we have the Rankine-Hugoniot condition (40) and the three surface equations at $r = a(u)$ mentioned above. Furthermore, expressions for $\Omega_{\rm I}$, $\Omega_{\rm II}$, and $\epsilon_{\rm II}$ can be obtained from equations (2)–(5), and equation (40) implies (see Appendix) that

$$\dot{C} = \frac{-T + \lambda\sqrt{T^2 - 4\Sigma\Xi}}{2\Sigma}, \tag{41}$$

where $\lambda = \pm 1$. It will be shown in the next section that there is a conspicuous relation between λ and the sign of the anisotropic jump across the shock ($\Delta = h - k$).

As in our previous work, the luminosity E has been assumed to be a Gaussian such that the total radiated energy is a fraction of the initial mass. Finally, $\epsilon_{\rm I}$ and $\epsilon_{\rm II}$ are related via a constant "opacity" parameter α as

$$\epsilon_{\rm I} = \alpha\epsilon_{\rm II}\ . \tag{42}$$

It is important to note that, in contrast to the composite isotropic sphere, a pulse is not assumed at the shock front ($r = c + 0$) because $\epsilon_{\rm II}$ can be solved from the field equations. This remarkable difference, being a clear physical consequence of the earlier supposition (31), separates the system of surface equations into two blocks: the first group corresponds to equations (25), (27), and (29), which involve only quantities evaluated at $r = a(u)$; equation (41) completes the system, providing the evolution of the shock front within the matter configuration. This apparently simplifying separation leads to a computationally more expensive solution of the system of surface equations because, for every integration step, it will become necessary to compute β, $\tilde{m}$, and their derivatives at $r = c(u)$ and then calculate $\epsilon_{\rm II}$.

Surface equations are integrated for several sets of initial data and physical parameters. Among those sets we have established two standards differing only in the opacity: the "standard radiant set" (SRS) and the "standard opaque set" (SOS) having $\alpha = 0.90$ and $\alpha = 1.10$, respectively. Both share common values for other physical parameters and initial data. Specific departures from SOS and SRS quantities will be explicitly indicated; otherwise the following values are assumed:

$$A|_{u=0} = 10.0\ , \qquad \Omega|_{u=0} = 0.857\ ,$$
$$F|_{u=0} = 0.8\ , \qquad C|_{u=0} = 6.0\ ,$$
$$\text{Peak at } u = 15.0\ , \qquad \sigma = 3.0\ .$$

The radiated energy is one-tenth of the total initial mass, and the variance of the pulse, σ, is used as a width indicator.

The integration time interval is suggested by the behavior of the matter variables themselves. Figures 2*a*–2*d* display the profiles of these variables for a particular anisotropic configuration in an SRS. They have been monitored at four different mass shells, $r/a = 0.2$, 0.4, 0.6, 0.8 (*continuous lines*) and at either side of the shock front (*dotted lines*). Figure 3 exhibits the influence of the anisotropic jump for SOS spheres configured with anisotropic cores and isotropic mantles. The relevance of the "radiance" $\chi = 1 - \alpha$ of the shock may be appreciated in Figure 4. Figure 5 contains the shock evolution for different inner core masses having $\Delta = 0.25$; SOS cases are represented by continuous lines, while SRS are represented by dotted ones. The evolution of the core for several emitted pulses is sketched in Figures 6*a* and 6*b*. We defer a detailed discussion of the results to the next section.

V. DISCUSSION OF THE RESULTS

Before discussing the results themselves, we would like to emphasize the most important features which establish the scheme outlined above as a consistent and workable framework in general relativistic radiating hydrodynamics.

The matter distribution considered is free of singularities everywhere. The Rankine-Hugoniot relations match, through the shock, the inner and the outer solutions, and the junction conditions across the boundary surface fulfill the remaining coupling with the radiating version of the Schwarzschild exterior solution (the Vaidya solution). A heuristic assumption relating pressure, energy density, and the radial velocity of matter leads (via the junction conditions at the boundary and Rankine-Hugoniot relations) to a system of ordinary differential equations for quantities evaluated at either the boundary surface or the shock front. This *Ansatz*, chosen on a solid physical ground, is related to the Schwarzschild anisotropic interior solution, which is considered one of the stiffest equations of state for ultradense matter, since it describes the homogeneous Schwarzschild incompressible fluid in the static and isotropic limit.

Using the method described above, we are able to work out explicit models and to display the most important aspects in the evolution of a composite anisotropic sphere. As will become clear from the discussion below, the presence of the two phases strongly conditions the motion of the interface (the shock), and this motion will reflect the dominance of one anisotropic phase over the other.

It can be noted from the evolution of the physical variables (Figs. 2*a*–2*d*) that a static configuration is reached by this sphere. This should not be taken as a particular property of this arbitrarily selected configuration; instead, it should be considered as a general result emerging from any of the models obtained. It is also apparent from these figures that a weak shock delimits the core of this nearly homogeneous sphere. This can be understood bearing in mind that the effective variables are continuous across the shock, and, in the very stable configurations considered, the effective variables become similar to the physical ones. It is worthwhile noticing that at a given mass shell, during the emission of the pulse ($12 < u < 18$), the density remains almost constant while the pressure rises, and a significant flux of energy is present across it.

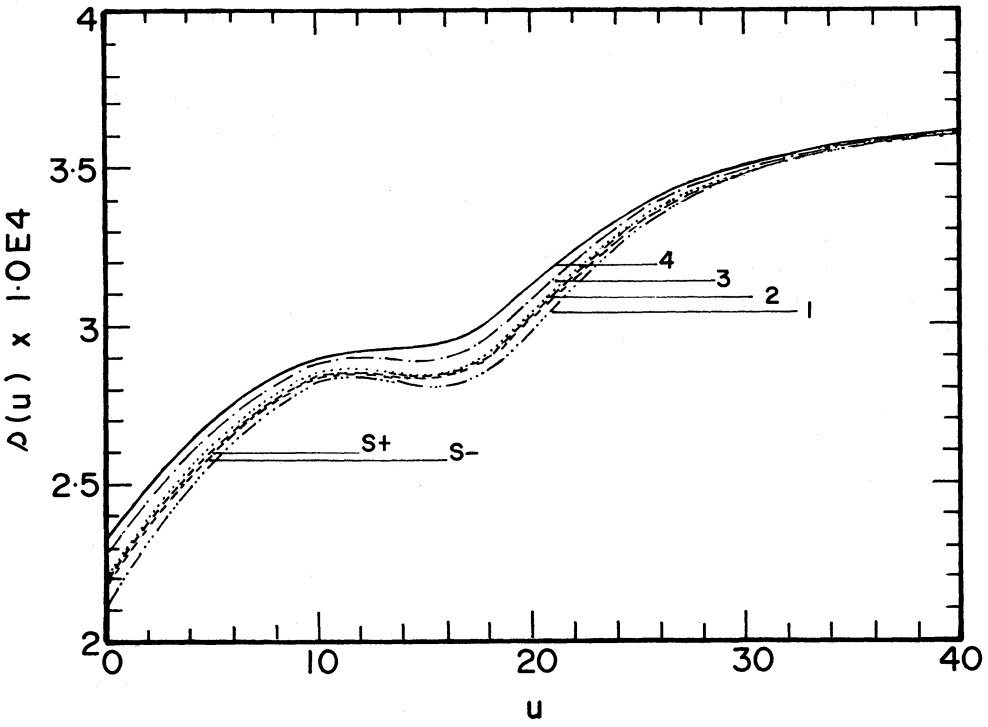

FIG. 2*a*

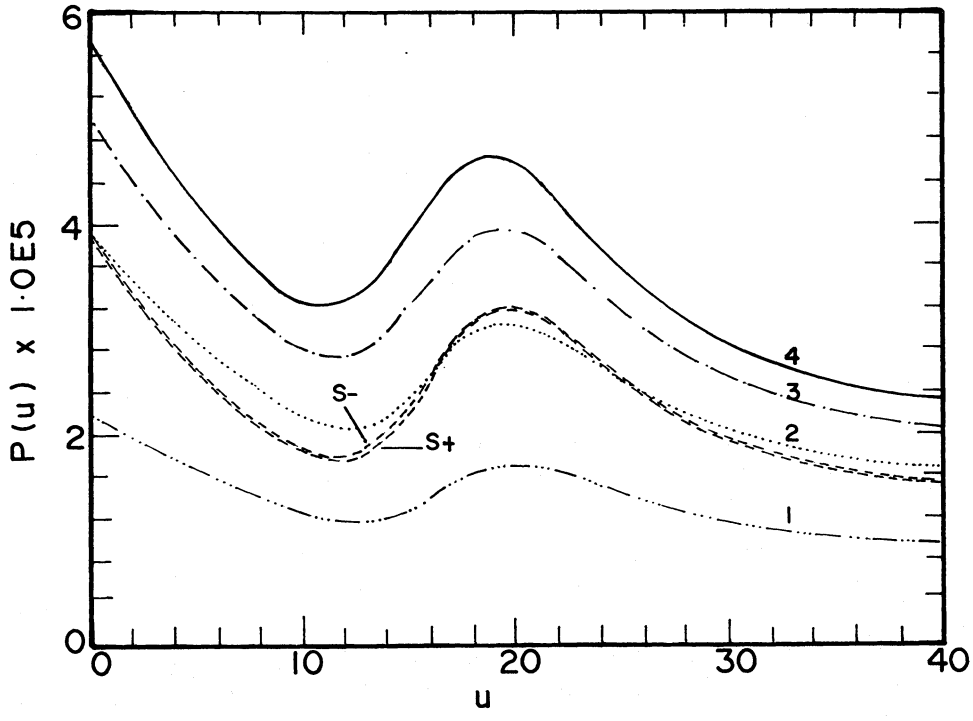

FIG. 2*b*

FIG. 2.—Evolution of the physical variables. This SRS model is configured with a $k\uparrow$ core and an isotropic mantle having $\Delta = 0.25$. The evolution of (*a*) density, (*b*) pressure, (*c*) mass velocity, and (*d*) energy flux are monitored at four different mass shells and at both sides of the shock front. The labels S_+ (region II) and S_- (region I) denote their values measured on the shock front; curves corresponding to the ratio $r/a = 0.2, 0.4, 0.6, 0.8$ are respectively labeled as 4, 3, 2, 1.

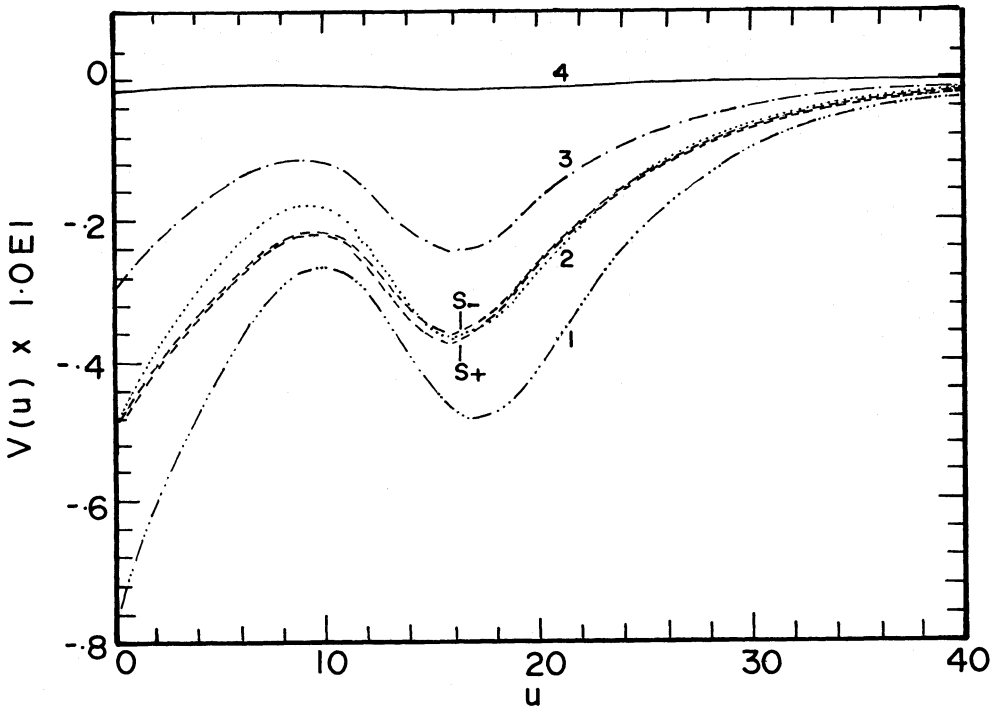

FIG. 2c

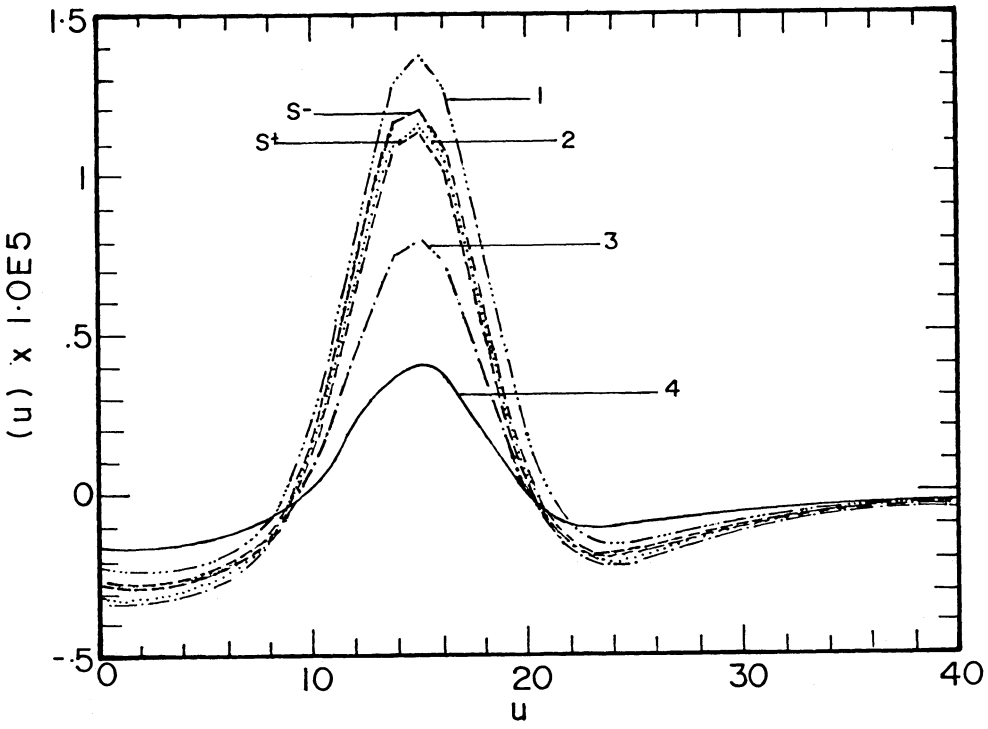

FIG. 2d

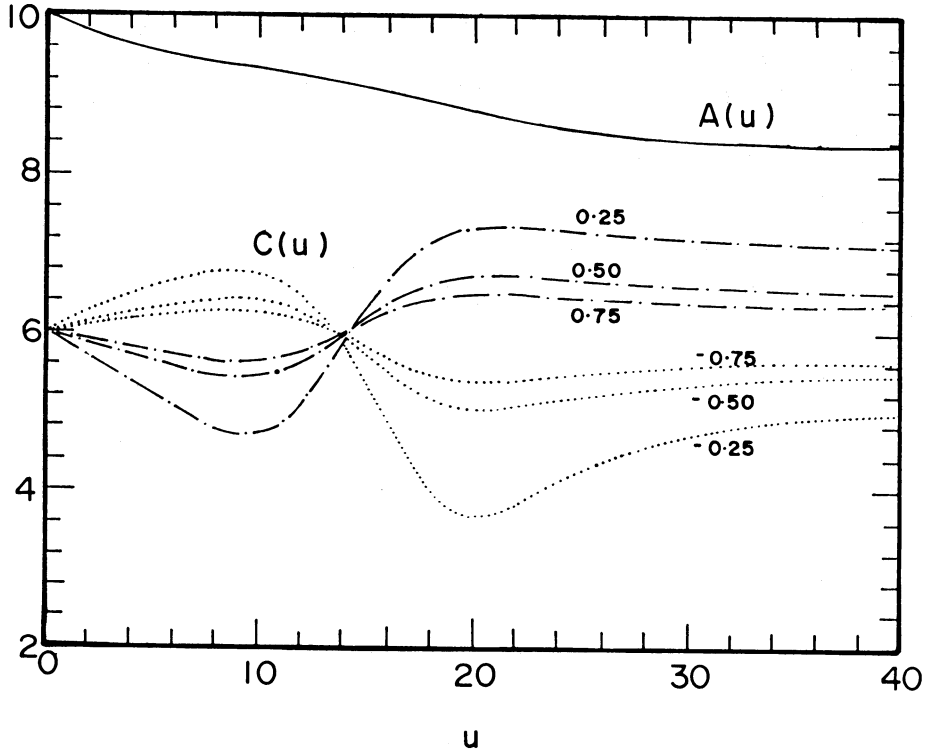

FIG. 3.—Influence of the anisotropic jump (SOS). Models are configured having $k\uparrow$ cores and isotropic mantles ($\Delta > 0.0$), and $k\downarrow$ cores and isotropic mantles ($\Delta < 0.0$). Curves are labeled with the corresponding values of the anisotropic jump Δ.

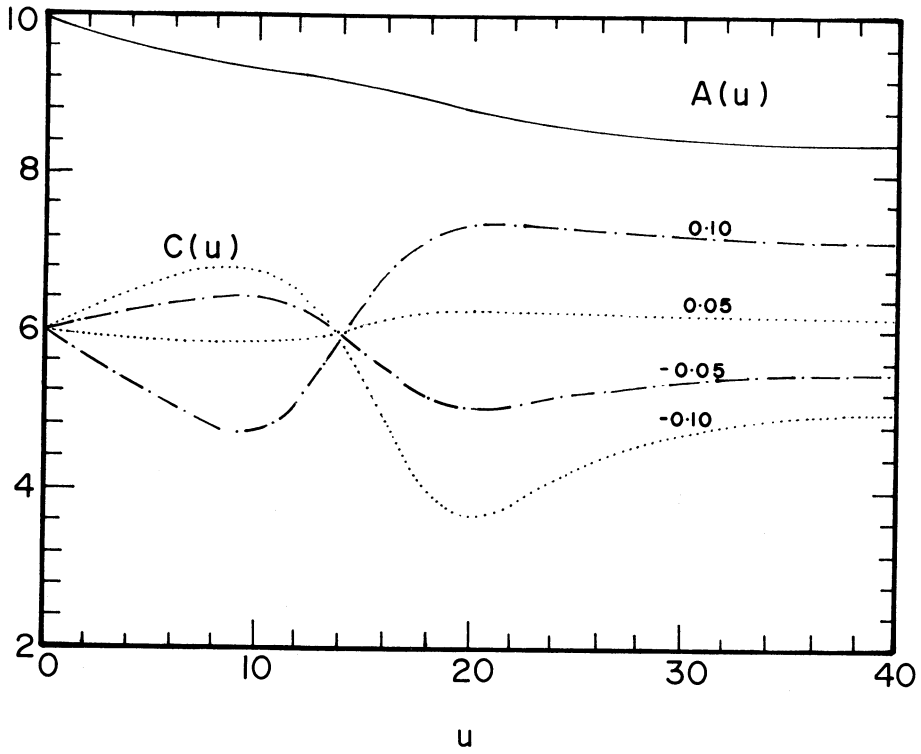

FIG. 4.—Influence of the shock radiance. Models are configured with $k\uparrow$ core and isotropic mantle having $\Delta = 0.25$. Curves are labeled with the corresponding values of the shock "radiance."

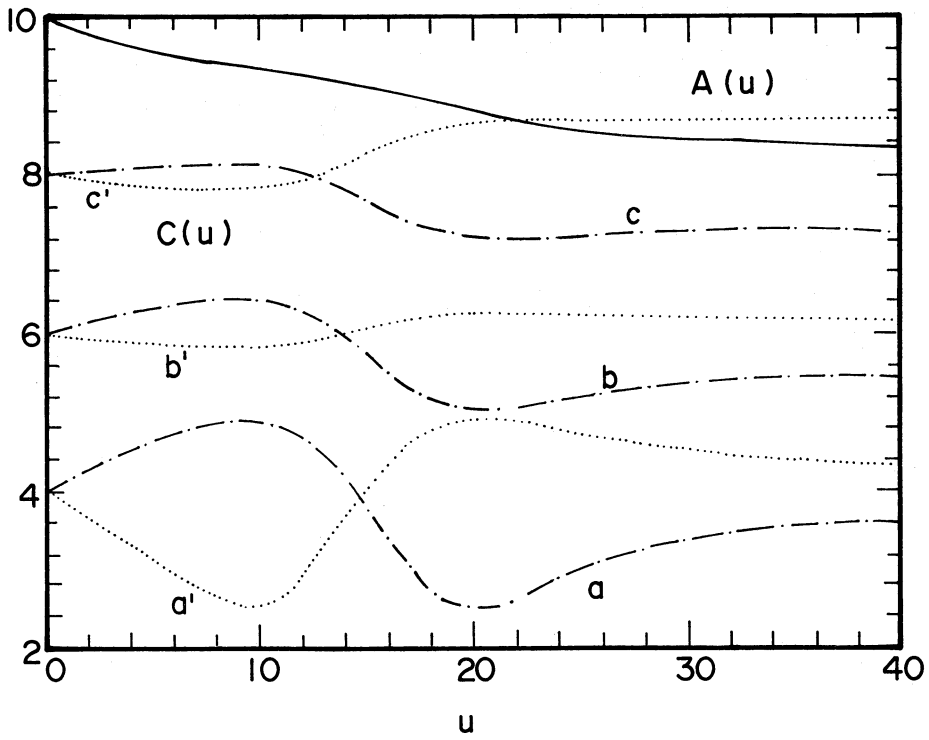

FIG. 5.—Influence of the core mass for models having $\Delta = 0.25$, with $k\uparrow$ cores and isotropic mantles. Unprimed labels *a*, *b*, and *c* (*continuous lines*) correspond to SOS models with initial radii 4, 6, and 8, respectively, while primed labels (*a'*, *b'*, and *c'*) represent SRS spheres with the same initial radius configuration.

The evolution of the shock is characterized by two distinctive features: the anisotropic jump across the shock ($\Delta = h - k$) and the "radiance" of the shock. Figure 3 exhibits the influence of the anisotropic jump for SOS spheres configured with anisotropic cores and isotropic mantles. Curves representing the case of SRS spheres coincide with the equivalent ones for the SOS case by changing the signs of its anisotropic jumps, and are not sketched.

The anisotropic jump across the shock Δ indicates how different in anisotropy the two coexisting phases are, and it also portrays the relevance of a particular anisotropic configuration for the evolution of the shock. Specifically, it can be appreciated from Figure 3 that violent shock motions are enhanced by feeble anisotropic phase transitions ($\Delta = \pm 0.25$) while a more marked difference in anisotropy between the phases ($\Delta = \pm 0.75$) inhibits the evolution of the nucleus. This result resembles in many aspects those reported earlier by Takahara and Sato (1985) in a different context. These authors carried out systematic simulations of gravitational collapses where, by taking into account the general relativistic effects, the influence of the phase transition on a supernova explosion became clear.

The other parameter that decisively affects the evolution of composite anisotropic spheres is the shock luminosity, which, incorporated in our scheme through the "radiance" of the shock wave front χ (or, equivalently, via its "opacity" α), could represent a radiating shock when $\chi > 0$ or an opaque one using $\chi < 0$. In connection with this question, one may observe that ϵ_{II} is not given by hand, but, instead, its value is calculated via the Einstein equation. The resemblance in the model evolution for SOS and SRS configurations after changing the sign of the anisotropic jump brings out the relevance of the product of both "radiance" and anisotropic jump for characterizing the propagation of the shock. In Figure 4 the model evolutions with different "radiances" are sketched; it can be inferred that the more radiating the shock, the deeper it recedes, and, as in our previous work, deeper recessions seem to be associated with the more violent expansions. Opaque shocks expand in early epochs, but after the pulse is emitted they stall.

The conclusion drawn from Table 1 is again the decisive influence of the anisotropic jump and the shock "radiance" on the evolution of the core. Additionally, there also emerges a conspicuous relation among the signs of λ, Δ, and χ; the sign of the anisotropy difference between the two phases seems to indicate which set of surface equations will govern the model, i.e., the sign of λ and the subsequent evolution will be determined by the sign of the radiance. In this table, $k\uparrow$, $k\downarrow$, $h\uparrow$, and $h\downarrow$ indicate $k > 1$, $k < 1$, $h > 1$, and $h < 1$, respectively, while I represents the isotropic phase, i.e., $k = 1$ or $h = 1$, depending on the region described. It is important to keep in mind that models having $k\downarrow$ or $h\downarrow$ entail greater redshifts than the corresponding isotropic $k\uparrow$ or $h\uparrow$ phase configurations.

We have also found that the configurations studied are particularly sensitive to the change of two other parameters, namely, the mass of the inner core and the intensity of the emitted pulse of radiation. Again, curves representing the shock evolution for models having $\Delta = -0.25$ coincide with those having $\Delta = 0.25$ by changing the signs of the "radiance," and are not presented.

Figure 5 shows the extent to which a larger nucleus affects the evolution of composite anisotropic spheres. There it is apparent that massive cores enhance gravitational attraction, and this inhibits violent shock propagations. In contrast, lighter nuclei present dramatic changes in the shock motions. It is worthwhile noticing that under certain conditions the shock may reach the surface of

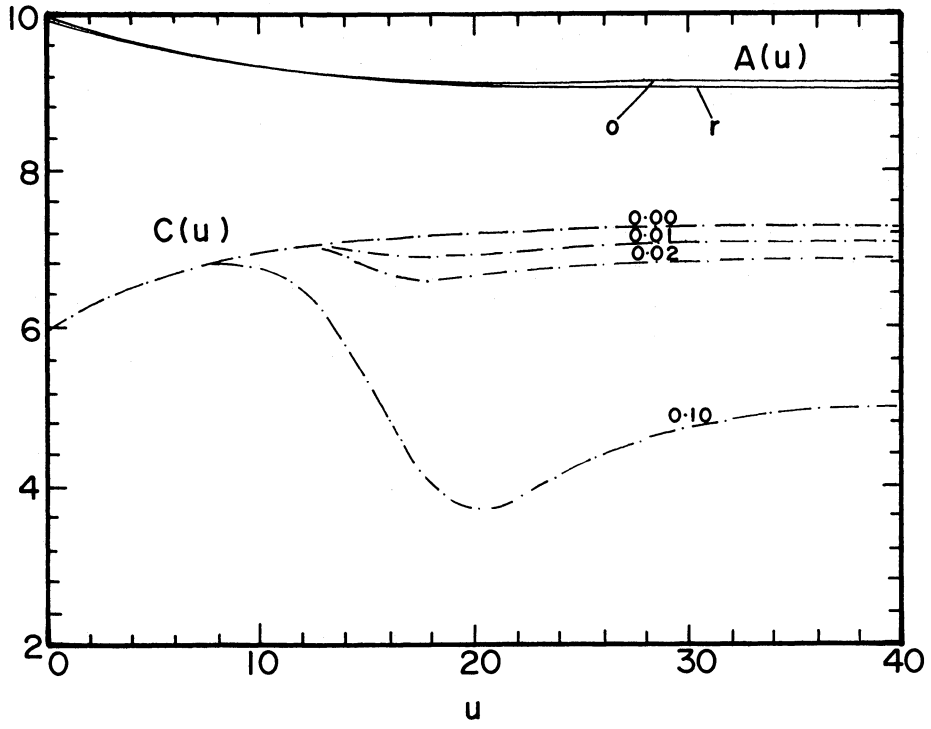

FIG. 6a

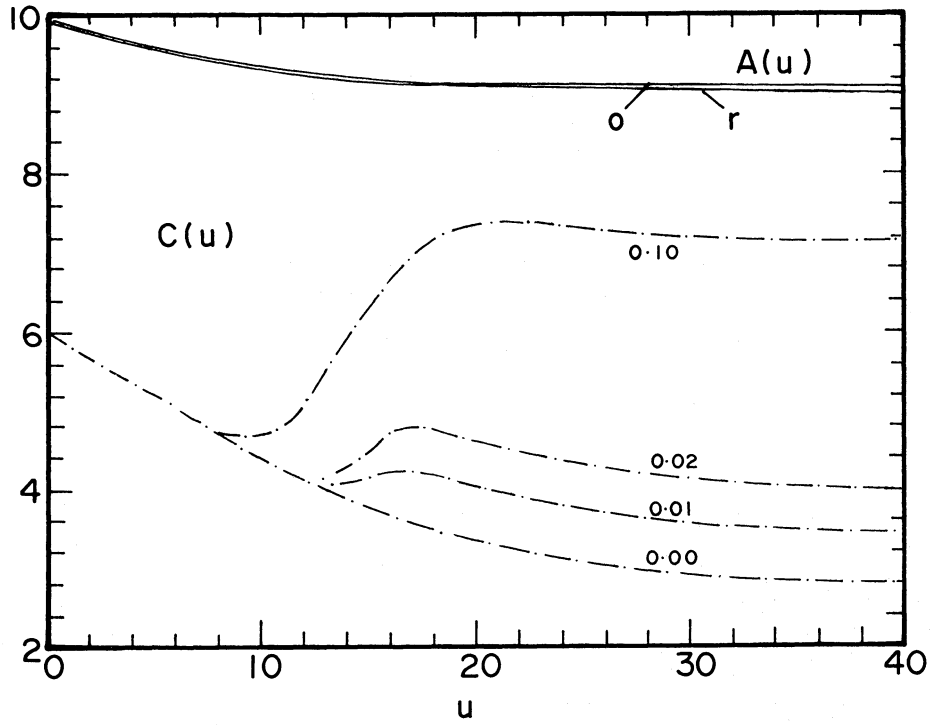

FIG. 6b

FIG. 6.—Influence of the radiation pulse. (*a*) SRS emitted energy; (*b*) SOS emitted energy. Models are configured with $k\downarrow$ cores and isotropic mantles and with $\Delta = 0.25$. Curves are labeled with the corresponding fractions of the initial mass radiated. Expanding cores of the opaque model (curve 0.00) represented in (*a*) shrink as greater pulses are emitted (curves 0.01, 0.02, and 0.10). In (*b*) the eroding nucleus of the opaque sphere turns out to be expanding (curve 0.00) when a pulse of radiation is present (curves 0.01, 0.02, and 0.10).

TABLE 1

RELATION AMONG THE SIGNS OF THE EVOLUTION PARAMETERS

Sphere Configuration			Sign of the Evolution Parameters			
					Core Evolution (opaque sphere)	
Core		Mantle	Δ	λ	Expansive χ	Shrinking χ
$k\downarrow$	$>$	$h\downarrow$	+	+	+	−
$k\downarrow$	$<$	$h\downarrow$	−	−	−	+
$k\downarrow$		I	−	−	−	+
$k\downarrow$		$h\uparrow$	−	−	−	+
I		$h\downarrow$	+	+	+	−
I		$h\uparrow$	−	−	−	+
$k\uparrow$		$h\downarrow$	+	+	+	−
$k\uparrow$		I	+	+	+	−
$k\uparrow$	$<$	$h\uparrow$	−	−	−	+
$k\uparrow$	$>$	$h\uparrow$	+	+	+	−

the sphere; that is to say, an anisotropic phase may dominate over the other, and a one-phase sphere could be obtained. These configurations are found to have $\Delta > 0$ and $\chi > 0$ or $\Delta < 0$ and $\chi < 0$.

The energy emitted by the pulse also influences the evolution of the spheres (Figs. 6*a* and 6*b*). Opaque models having either $\Delta > 0$ and $\chi > 0$ or $\Delta < 0$ and $\chi < 0$ drastically change the expansion of their nuclei by the emission of the pulse, while in models with opposite sign combinations of Δ and χ the shocks seem to be driven outward by the radiation.

The general hydrodynamic picture described could emerge as a probable scenario for collapsing configurations where phase transitions are thought to play important roles. Certain stages in a supernova outburst and the subsequent birth of a neutron star (Burrows and Latimer 1986), strongly conditioned by the inner core evolution, suggest the possible relevance of some of the results obtained. Again, the combined effect of general relativity and a softening of the equation of state at high density has dramatic influences on the propagation of the shock wave front (Baron, Cooperstein, and Kahana 1985; Takahara and Sato 1985). All the conclusions sketched above are still valid for any of the anisotropic configurations coming from Table 1, although we have presented here only spheres involving anisotropic and isotropic phases. Apart from its simplicity, the reason for this presentation was the astrophysical interest on the conditions which make the anisotropic phase dominant.

We would like to conclude with the following comment: we have again considered that the most relevant observable in a collapse process should be the profile of the neutrino luminosity, and this is the reason for explicitly giving the function E. However, from a formal point of view it would be justifiable to choose any other function of u (A, Ω, C, etc.). We would welcome the opinion of specialists on this point.

One of us (L. H.) gratefully acknowledges the financial support from Fundación Polar. We would also like to thank the Centro Científico IBM de Venezuela, where part of the computational work was carried out, and especially C. Mendoza, M. Luna, and C. Ribeiro for their helpful advice. This work has been partially supported by the Consejo de Desarrollo Científico y Humanístico de la Universidas de Los Andes, Mérida, under project C 187-82.

APPENDIX

I. EVALUATION OF β, $\tilde{m}$, AND THEIR DERIVATIVES

We present here the expressions for the metric functions and their derivatives. A comma has been used to denote differentiation with respect to u and r (suffixes 0 and 1, respectively). For the core we have stated that

$$\beta_{\rm I} = \frac{1}{2k}\ln\left|\frac{Y}{2}\right| + \frac{1}{2h}\ln\left|\frac{\tilde{\rho}(3-2\Omega)}{\Omega(\tilde{\rho}+3\tilde{P}_+)^{h/2}}\right|, \tag{A1}$$

where

$$Y = \frac{3(\tilde{\rho}+\tilde{P}_+)(W^2-C^2)^{k/2} - (\tilde{\rho}+3\tilde{P}_+)(W^2-r^2)^{k/2}}{\tilde{\rho}(W^2-r^2)^{k/2}},$$

and, as before,

$$\tilde{P}_+ = \tilde{\rho}\,\frac{(3-2\Omega)(W^2-C^2)^{h/2} - (W^2-A^2)^{h/2}}{3(W^2-A^2)^{h/2} - (3-2\Omega)(W^2-C^2)^{h/2}}.$$

Thus, its derivatives with respect to r should become

$$\beta_{\rm I,\,1} = \frac{3r(\tilde{\rho}+\tilde{P}_+)(W^2-C^2)^{k/2}}{2\tilde{\rho}Y(W^2-r^2)^{1+k/2}} \tag{A2}$$

and

$$\beta_{\mathrm{I},11}=\frac{\beta_{\mathrm{I},1}}{r(W^2-r^2)}\left[(W^2+r^2)-k\frac{r^2(\tilde{\rho}+3\tilde{P}_+)}{Y}\right]. \tag{A3}$$

It will be suitable to express $\beta_{\mathrm{I},01}$ in the following form:

$$\beta_{\mathrm{I},01}=\beta_{\mathrm{I},1}(\tau_a\dot{A}+\tau_f\dot{F}+\tau_c\dot{C}+\tau_\omega\dot{\Omega}), \tag{A4}$$

with the corresponding coefficients written as

$$\tau_a=\frac{W^2}{A(W^2-r^2)}\left(\frac{\tilde{\rho}+3\tilde{P}_+}{\tilde{\rho}Y}\frac{r^2-C^2}{W^2-C^2}-2\right)-\frac{hC^2(\tilde{\rho}+3\tilde{P}_+)}{\tilde{\rho}AY(W^2-C^2)},$$

$$\tau_f=\frac{W^4}{2A^2(W^2-r^2)}\left(\frac{\tilde{\rho}+3\tilde{P}_+}{\tilde{\rho}Y}\frac{r^2-C^2}{W^2-C^2}-2\right)-\frac{hA^2(\tilde{\rho}+3\tilde{P}_+)(A^2-C^2)}{2\tilde{\rho}Y(W^2-C^2)(W^2-A^2)},$$

$$\tau_c=\frac{C(\tilde{\rho}+3\tilde{P}_+)}{\tilde{\rho}Y(W^2-C^2)}(k-h),\qquad \tau_\omega=\frac{-2(\tilde{\rho}+3\tilde{P}_+)}{Y\tilde{\rho}(3-2\Omega)}.$$

For the outer region we have obtained

$$\beta_{\mathrm{II}}=\frac{1}{2h}\ln\left|\frac{X}{2\Omega}\right|, \tag{A5}$$

using

$$X=\frac{3(W^2-A^2)^{h/2}-(3-2\Omega)(W^2-r^2)^{h/2}}{(W^2-r^2)^{h/2}}.$$

Its derivatives could be expressed as

$$\beta_{\mathrm{II},1}=\frac{3r(W^2-A^2)^{h/2}}{2X(W^2-r^2)^{1+h/2}} \tag{A6}$$

and

$$\beta_{\mathrm{II},11}=\frac{\beta_{\mathrm{II},1}}{r(W^2-r^2)}\left[W^2+r^2-h\frac{r^2(3-2\Omega)}{X}\right]. \tag{A7}$$

Also $\beta_{\mathrm{I},01}$ will be shaped as

$$\beta_{\mathrm{II},01}=\beta_{\mathrm{II},1}(\bar{\tau}_a\dot{A}+\bar{\tau}_f\dot{F}+\bar{\tau}_c\dot{C}+\bar{\tau}_\omega\dot{\Omega}), \tag{A8}$$

and the corresponding coefficients can be written as

$$\bar{\tau}_a=\frac{W^2}{A(W^2-r^2)}\left[\frac{h(3-2\Omega)}{X}\frac{r^2-A^2}{W^2-A^2}-2\right]-\frac{hA(3-2\Omega)}{X(W^2-A^2)},$$

$$\bar{\tau}_f=\frac{W^4}{2A^2(W^2-r^2)}\left[\frac{h(3-2\Omega)}{X}\frac{r^2-A^2}{W^2-A^2}-2\right],\qquad \tau_\omega=-\frac{2}{X}.$$

II. THE EQUATION FOR THE SHOCK EVOLUTION

We sketch here some of the intermediate calculations that lead up to equation (41). From the Rankine-Hugoniot condition (40),

$$\Omega_{\mathrm{II}}(\Omega_{\mathrm{II}}-1)-\Omega_{\mathrm{I}}(\Omega_{\mathrm{I}}-1)=-\frac{1}{\tilde{\rho}_c+\tilde{P}_c}[\epsilon]_c, \tag{A9}$$

Using equations (3), (4), and (5) Ω_{I} and Ω_{II} can be expressed as

$$\Omega_s=\left\{\frac{\tilde{m}_{s,1}}{4\pi c^2}-\frac{\beta_{s,01}}{4\pi}e^{-2\beta_s}+\frac{1}{8\pi}\left(1-\frac{2\tilde{m}_s}{c}\right)\left[2\beta_{s,11}+4(\beta_{s,1})^2-\frac{\beta_{s,1}}{c}\right]\right\}\left[\frac{\beta_{s,1}}{2\pi c}\left(1-\frac{2\tilde{m}_s}{c}\right)\right]^{-1}$$
$$+\frac{3(1-2\tilde{m}_{s,1})-\tilde{m}_{s,11}}{4\beta_{s,1}(1-2\tilde{m}_s/c)}-\frac{\pi 2\xi_s(\tilde{P}+\tilde{\rho})(4\pi C^3\tilde{P}+\tilde{m})}{\beta_{s,1}(1-2\tilde{m}_s/c)^2}, \tag{A10}$$

$s=\mathrm{I},\mathrm{II}$ indicating the region they belong to. (Note: a misprint in eq. [A3] in Herrera and Núñez 1987 caused a $\beta_{s,1}$ to be missing in the denominator of the second term. The last term represents the anisotropic contribution in eq. (A10), where ξ is the parameter

used in eq. [13] to characterize the anisotropy of the configuration. Here, we have also used a comma to denote differentiation, in order to avoid any possible confusion with subscripts.)

Substituting in equation (A10) the corresponding expressions for β_s, $\beta_{s,1}$, $\beta_{s,11}$, $\beta_{s,01}$, $\tilde{m}_s$, $\tilde{m}_{s,1}$, and $\tilde{m}_{s,11}$ in terms of the dimensionless variables, we can shape these equations in the following form:

$$\Omega_{\rm I} = \Lambda\dot{C} + \Phi\,, \qquad \Omega_{\rm II} = \Phi;$$

thus, we can obtain from equation (A9)

$$\Sigma\dot{C}^2 + T\dot{C} + \Xi = 0 \leftrightarrow \dot{C} = -\frac{T \pm \sqrt{T^2 - 4\Sigma\Xi}}{2\Sigma}\,,$$

where

$$\Sigma = \Lambda^2\,, \qquad T = \Lambda(2\Phi - 1)\,, \qquad \Xi = -\frac{1}{\tilde{\rho}_c + \tilde{P}_c}\,[\epsilon]_c = -\frac{8\pi\chi\epsilon_{\rm II}\tilde{\rho}}{3(\tilde{\rho} + \tilde{P}_+)}$$

and

$$\Phi = \Gamma_a\dot{A} + \Gamma_f\dot{F} + \Gamma_\omega\dot{\Omega} + 1\,.$$

The coefficients can be written as

$$\Gamma_a = \Gamma_0\frac{W}{A}\left\{W - \frac{h(\tilde{\rho} + 3\tilde{P}_+)}{\tilde{\rho}(W^2 - A^2)}\,[A(1-F)^{1/2}(W^2 - C^2) + W(C^2 - A^2)]\right\},$$

$$\Gamma_f = \Gamma_0\frac{W^4}{2A^2}\left[1 - \frac{h(\tilde{\rho} + 3\tilde{P}_+)(C^2 - A^2)}{4\tilde{\rho}(W^2 - A^2)}\right],$$

$$\Gamma_\omega = \Gamma_0\frac{(\tilde{\rho} + 3\tilde{P}_+)(W^2 - C^2)}{2\tilde{\rho}(3 - 2\Omega)}\,,$$

where

$$\Gamma_0 = -\frac{3C(\tilde{\rho} + \tilde{P}_+)}{2\tilde{\rho}(W^2 - C^2)^{1/2}}\left[\frac{\Omega(\tilde{\rho} + 3\tilde{P}_+)}{3 - 2\Omega}\right]^{1/h}.$$

REFERENCES

Baron, E., Cooperstein, J., and Kahana, S. 1985, *Phys. Rev. Letters*, **55**, 126.
Bayin, S. 1982, *Phys. Rev. D*, **26**, 1262.
Bondi, H. 1964, *Proc. Roy. Soc. London A*, **281**, 39.
Bowers, R. I., and Liang, E. P. T. 1974, *Ap. J.*, **188**, 657.
Burrows, A., and Latimer, J. M. 1986, *Ap. J.*, **307**, 178.
Canuto, V. 1973, in Proc. Solvay Conference on Astrophysics and Gravitation, Neutron Stars (Brussels), unpublished.
Collins, J. C., and Perry, M. J. 1975, *Phys. Rev. Letters*, **34**, 1353.
Cosenza, M., Herrera, L., Esculpi, M., and Witten, L. 1981, *J. Math. Phys.*, **22**, 118.
———. 1982, *Phys. Rev. D*, **25**, 2527.
Duggal, K. L. 1987, *J. Math. Phys.*, **28**, 2700.
Duggal, K. L., and Sharma, R. 1986, *J. Math. Phys.*, **27**, 2511.
Esculpi, M., and Herrera, L. 1986, *J. Math. Phys.*, **27**, 2087.
Haensel, P., and Prószyński, M. 1980, *Phys. Letters*, **96B**, 233.
Hartle, J. B., Sawyer, R. F., and Scalapino, D. J. 1975, *Ap. J.*, **199**, 471.
Heintzmann, H., and Hillebrandt, W. 1975, *Astr. Ap.*, **38**, 51.
Herrera, L., and Jiménez, J. 1983, *Phys. Rev. D*, **28**, 2987.
Herrera, L., Jiménez, J., Leal, L., Ponce de León, J., Esculpi, M., and Galina, V. 1984, *J. Math. Phys.*, **25**, 3274.
Herrera, L., Jiménez, J., and Ruggeri, G. 1980, *Phys. Rev. D*, **22**, 2305.
Herrera, L., and Núñez, L. 1987, *Ap. J.*, **319**, 868.
Herrera, L., and Ponce de León, J. 1985*a*, *J. Math. Phys.*, **26**, 2018.
———. 1985*b*, *J. Math. Phys.*, **26**, 2302.
Herrera, L., Ruggeri, G., and Witten, L. 1979, *Ap. J.*, **234**, 1094.
Hillebrandt, W., and Steinmetz, K. O. 1976, *Astr. Ap.*, **53**, 283.
Ibáñez, J. M. 1984, *Ap. J.*, **284**, 381.
Ibáñez, J. M., and Miralles, J. A. 1985, *Ap. J.*, **299**, 21.
Itoh, N. 1970, *Progr. Theoret. Phys.*, **44**, 291.
Kampfer, B. 1985, *Phys. Letters*, **153B**, 121.
Krori, K. D., Borgohain, P., and Devi, R. 1984, *Canadian J. Phys.*, **62**, 239.
Letelier, P. S. 1980, *Phys. Rev. D*, **22**, 807.
Maartens, R., Mason, D. P., and Tsamparlis, M. 1986, *J. Math. Phys.*, **28**, 1114.
Maxwell, O. V. 1987, *Ap. J.*, **316**, 295.
Maxwell, O. V., Brown, G. E., Campbell, D. K., Dashen, R. F., and Manassah, J. T. 1977, *Ap. J.*, **216**, 77.
Migdal, A. B. 1971, *Soviet Phys.—JETP*, **34**, 1184.
Migdal, A. B., Chernoutsan, A. I., and Mishustin, I. N. 1979, *Phys. Letters*, **83B**, 158.
Ponce de León, J. 1987, *J. Math. Phys.*, **28**, 1114.
Ram, S., and Pandey, J. 1986, *Astr. Space Sci.*, **127**, 9.
Ruderman, M. 1972, *Ann. Rev. Astr. Ap.*, **10**, 427.
Sawyer, R. F. 1972, *Phys. Rev. Letters*, **29**, 382.
Sawyer, R. F., and Scalapino, D. J. 1973, *Phys. Rev. D*, **7**, 953.
Sawyer, R. F., and Soni, A. 1977, *Ap. J.*, **216**, 73.
Sokolov, A. I. 1980, *Soviet Phys.—JETP*, **52**, 575.
Takahara, M., and Sato, K. 1985, *Phys. Letters*, **156B**, 17.
Taub, A. H. 1948, *Phys. Rev.*, **74**, 328.
———. 1983, in *Proc. Third Marcel Grossman Meeting on General Relativity*, ed. H. Ning (Amsterdam: North-Holland; Beijing: Science), p. 165.

LUIS HERRERA: Apartado 80793, Caracas 1080A, Venezuela

LUIS NÚÑEZ: Apartado 69649, Caracas 1063A, Venezuela